Penetration Fracture of Sea Ice Plate: Simplified Analysis and Size Effect

By Zdeněk P. Bažant,[1] Fellow, ASCE, and Yuan-Neng Li[2]

Abstract: Vertical penetration of an object through a floating elastic-brittle plate from the bottom up or the top down is studied. Based on field observations, it is assumed that many symmetric cracks grow radially from a small loaded area, and the maximum load is achieved at the initiation of circumferential cracks. Nevel's approximation, in which the plate wedges between the radial cracks are analyzed as narrow floating beams of linearly varying width, is adopted. This makes an analytical solution possible. The rate of energy release due to the radial crack growth is calculated according to linear elastic fracture mechanics and the theory of thin plates. This yields the dependence of the radial crack length on the load, which is considered to be uniformly distributed along a small circle. It is confirmed that there is a size effect such that the nominal stress (load divided by ice thickness squared) that causes similar cracks to grow is proportional to (ice thickness) $^{1/8}$ or, equivalently, to (flexural wavelengths) $^{1/2}$. However, the maximum load does not follow this size effect, because it is attained at the initiation of circumferential cracks, which is governed by a strength type of criterion and causes no size effect. When the size of the loaded area is fixed, there is a size effect due to an increase of load concentration, that is, a decrease of the ratio of the loaded circle diameter to the thickness. This size effect is intensified by the size dependence of the rupture modulus for bending, but in the normal size range, such a size effect is not significant. The relation between the length of the radial cracks and the applied load calculated by fracture mechanics is also useful for other methods of predicting the penetration load.

INTRODUCTION

This study deals with the penetration of a floating sea ice plate by a small object, either from the top down or the bottom up. This is an important problem in many respects, which has been analyzed by a number of investigators (Hertz 1984; Bernstein 1929; Korunov 1939; Assur 1956; Nevel 1958; Kerr 1975). Of main interest is the maximum force required for the penetration of the object. This force has been calculated according to the strength theory, either in the form of elasticity with a strength limit or in the form of plastic limit analysis. However, ice is a brittle—or, more precisely, quasi-brittle—material, and as experience indicates the mode of failure consists of cracking. In such a case, solution according to the strength theory would be appropriate if the maximum load were achieved right at the first crack initiation. Observations indicate that this is not the case. The maximum load is typically achieved only after extensive crack growth [as pointed out by Frankenstein (1963), and also reviewed by Kerr (1975)]. In such a case, the analysis should correctly be carried out according to fracture mechanics. The most important difference between fracture mechanics and the strength theory is the size effect. Its understanding is important for the interpretation of experimental observations, and especially for the extrapolation of reduced-scale tests.

[1]Walter P. Murphy Prof. of Civ. Engrg., Northwestern Univ., Evanston, IL 60208.
[2]Res. Asst. Prof., Dept. of Civ. Engrg., Northwestern Univ., Evanston, IL.

Note. Discussion open until November 1, 1994. To extend the closing date one month, a written request must be filed with the ASCE Manager of Journals. The manuscript for this paper was submitted for review and possible publication on October 13, 1992. This paper is part of the *Journal of Engineering Mechanics*, Vol. 120, No. 6, June, 1994. ©ASCE, ISSN 0733-9399/94/0006-1304/$2.00 + $.25 per page. Paper No. 4943.

The objective of the present paper is to analyze the penetration problem according to fracture mechanics and study the size effect, extending a preliminary study by Bažant (1992a). The basic concepts and hypotheses are similar to those in a recent study of thermal bending fracture of floating sea ice plates by Bažant (1991).

As is well known from field observations, penetration through a floating ice plate begins by propagation of radial cracks. They grow in a stable manner as the load increases, and the maximum load is reached as circumferential cracks begin to form between the radial cracks. As the circumferential cracks develop, the load decreases at increasing displacement. The ice segment between two adjacent radial cracks may be considered to behave approximately as a wedge-shaped beam of a linearly increasing cross-sectional width. The wedge-beam approximation, which was introduced by Nevel (1958) and has been used in many studies not based on fracture mechanics, is exact only if there are infinitely many radial cracks, with infinitely small central angles. As has been confirmed by experimental studies [Nevel (1958), in his discussion with Heaps and Sterns], this approximation correlates well with the actual deflection pattern in the wedge up to a central angle of 60°, and remains a reasonable approximation up to 90°. The advantage of the narrow wedge–beam approximation is that the problem becomes one-dimensional. We use this approximation in the present study [another study (Li and Bažant 1994) will solve the actual two-dimensional problem], in which a comparison with experiment data is also given. The test data that exist in the open literature are insufficient to verify the size effect, because they do not cover a sufficient range of sizes for one and the same type of ice.

BASIC EQUATIONS OF WEDGE-BEAM APPROXIMATION

Consider an infinitely extending elastic plate of thickness h floating on water of specific weight ρ [Fig. 1(*a*)], which acts exactly as an elastic foundation of Winkler type. The differential equation of equilibrium of the wedge

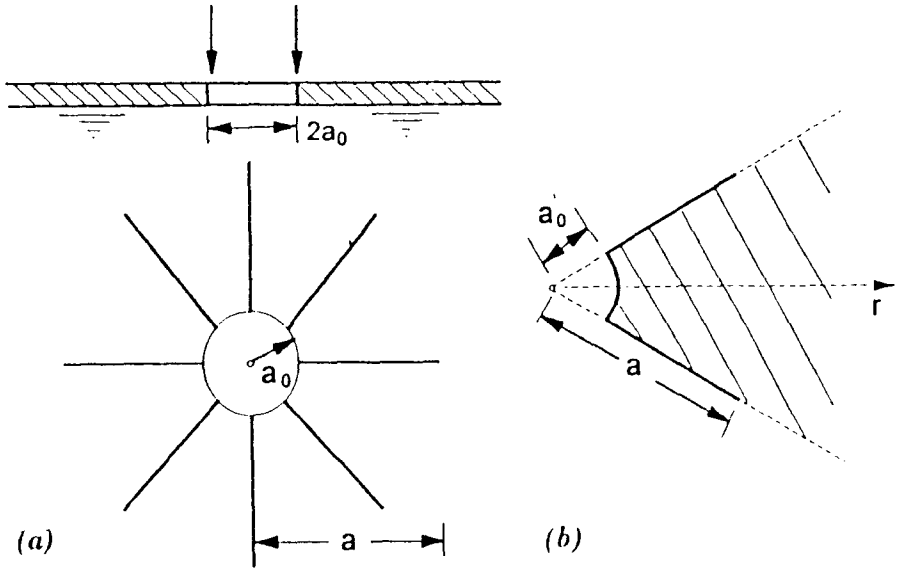

FIG. 1. (*a*) Floating Ice Sheet Subjected to Vertical Load; (*b*) Geometrical Definition of Wedge

beam shown in Fig. 1(*b*) may be written as $(EI_r w'')'' + p = 0$, in which w = downward deflection; E = Young's modulus; I_r = moment of inertia of the cross section; and p = vertical distributed force on the beam that is caused by buoyancy. The primes denote derivatives with respect to the radial coordinate r. Substituting $I_r = Ib$; $b = r\varphi_n$; and $p = \rho bw$, in which φ_n = central angle of the wedge beam; ρ = unit weight of seawater; and $I = h^3/12$ = moment of inertia of the plate cross section per unit width. We assume that the deflections are not so large that water would flood the top of the plate. Rearranging, we obtain the wedge-beam equation in the following form:

$$\frac{EI}{r}\frac{d^2}{dr^2}\left(r\frac{d^2w}{dr^2}\right) + \rho w = 0; \qquad a_0 < r < a \tag{1}$$

It is to be noticed that this equation is valid only at radial coordinates less than the length a of the radial cracks and larger than a certain small radius a_0 that cannot be taken smaller than approximately the thickness h of the plate. If the loading from the penetrating object is applied over an area larger than h, then a_0 is taken as the radius of the circle of which the loading is applied. Eq. (1) may alternatively be put in the form

$$EI\left(\frac{d^4w}{dr^4} + \frac{2}{r}\frac{d^3w}{dr^3}\right) + \rho w = 0 \tag{2}$$

Eq. (2) is written under the assumption that the beam width at radial coordinate r is equal to the arc length $\varphi_n r$. This is sufficiently accurate for small wedge angles. For larger angles, it would be more realistic to take the beam width as the chord length of the arc, i.e., $b = 2r\sin(\varphi_n/2)$. However, since (1) is homogeneous in b, such a modification would leave the equation unchanged (although it would affect the actual applied shear force for a given total load). At the same time, it would be somewhat more realistic to take the beam length coordinate as $r\cos(\varphi_n/2)$ instead of r, because r is measured along the radial cracks while the beam length should be measured along the axis of symmetry of the wedge. In practice, these corrections are unimportant (which will be confirmed by the subsequent paper).

It is convenient to introduce the length constant $l = (EI/\rho)^{1/4}$, which may be called the action radius. It characterizes the length over which the deflection due to a load at the tip of the wedge beam decays to a small value. In terms of the nondimensional coordinate $x = r/l$, (2) may be rewritten as

$$\frac{d^4w}{dx^4} + \frac{2}{x}\frac{d^3w}{dx^3} + w = 0; \qquad \alpha_0 < x < \alpha \tag{3}$$

in which the nondimensional limits of the range are $\alpha_0 = a_0/l$ and $\alpha = a/l$.

For radial coordinate r exceeding the crack length a, we assume the deformation of the infinite floating plate to be axisymmetric. The plate equation for axisymmetric bending is

$$D\left(\frac{d^2}{dr^2} + \frac{1}{r}\frac{d}{dr}\right)\left(\frac{d^2w}{dr^2} + \frac{1}{r}\frac{dw}{dr}\right) + \rho w = 0 \qquad a < r < \infty \tag{4}$$

in which $D = EI/(1 - \nu^2)$ is the plate bending stiffness of the elastic plate; and ν = Poisson's ratio. At $r = a$, the narrow wedge beams are assumed to be rigidly attached to the infinite plate, which means that the deflections and deflection slopes of the wedge beams and of the axisymmetric plate at $r = a$ are equal. It should be noted that the connection region between the wedge beams and the infinite plate is in a complex two-dimensional state. The continuity condition is just an approximation, which is, however, quite accurate when the central angle is small.

It is again convenient to introduce the length constant for the plate as $L = [EI/\rho(1 - \nu^2)]^{1/4} = \tau l$, where $\tau = (1 - \nu^2)^{-1/4}$; L may also be called the flexural wavelength because it represents the length over which an end disturbance in a semiinfinite plate decays to $e^{-\pi}$ of the end value. Using the nondimensional coordinate $X = r/L$, the governing differential equation for axisymmetric bending of an infinite plate on elastic foundation may be rewritten as

$$\left(\frac{d^2}{dX^2} + \frac{1}{X}\frac{d}{dX}\right)\left(\frac{d^2w}{dX^2} + \frac{1}{X}\frac{dw}{dX}\right) + w = 0 \qquad A < X < \infty \qquad (5)$$

in which $A = a/L = \alpha/\tau$.

METHOD OF SOLUTION

Both (2) and (5) are linear fourth-order ordinary differential equations with variable coefficients. Their general solutions are well known. The only problem is to set up the proper boundary conditions and continuity conditions at $x = \alpha$. For $x \geq \alpha$, the general solution of (5) that is bounded at infinity can be written as

$$w(X) = d_1 \ker(X) + d_2 \operatorname{kei}(X) \qquad (6)$$

where d_1 and d_2 = general constants; $\ker(X)$ and $\operatorname{kei}(X)$ = Kelvin functions, which are related to Bessel functions ber and bei. The deflection slope in nondimensional coordinate X may be defined as $\tilde{\theta} = dw/dX = L(dw/dr) = L\theta$, has the general expression

$$\tilde{\theta} = d_1 \ker'(X) + d_2 \operatorname{kei}'(X) \qquad (7)$$

in which the prime denotes the derivatives of ker and kei with respect to X. The constants can be solved in terms of the displacement and slope at the boundary point ($x = \alpha$ or $X = A$)

$$d_1 = \frac{\operatorname{kei}(A)}{\Delta} w_a - \frac{\operatorname{kei}(A)}{\Delta} \tilde{\theta}_a; \qquad d_2 = \frac{\ker(A)}{\Delta} w_a + \frac{\ker(A)}{\Delta} \tilde{\theta}_a \qquad (8a,b)$$

in which $\Delta = \ker(A)\operatorname{kei}'(A) - \ker'(A)\operatorname{kei}(A)$.

Furthermore, the nondimensional bending moment and shear force may be defined as:

$$\tilde{M} = \frac{ML^2}{D} = -\left(\frac{d^2w}{dX^2} + \frac{\nu}{X}\frac{dw}{dX}\right); \qquad \tilde{V} = \frac{VL^3}{D} = \frac{d^3w}{dX^3} + \frac{d}{dX}\left(\frac{1}{X}\frac{dw}{dX}\right) \qquad (9a,b)$$

However, $\tilde{M}$, $\tilde{V}$, and $\tilde{\theta}$ have the same dimension as the deflection w, which has the dimension of a length. Since all these equations depend linearly on

w, the actual dimension of w is not important in our study. For the purpose of simplicity, the term "nondimensional" is used in this paper with the specific meaning discussed here. In addition, the sign in our definition of the nondimensional shear force differs from the conventional definition. The purpose of dropping the negative sign is that the shear force in a cross section with its normal in the negative r-direction would be in the positive direction of deflection, so that the corresponding work be positive.

Combining (6) and (9), we can deduce the stiffness relation of the bending moment and the shear force to the deflection and the slope at the boundary point $r = a$

$$\bar{M}_a = k_{11}\bar{\theta}_a + k_{12}w_a \tag{10a}$$

$$\bar{V}_a = k_{21}\bar{\theta}_a + k_{22}w_a \tag{10b}$$

The stiffness coefficients are expressed as follows:

$$k_{11} = \left(\mathrm{ker}'' + \frac{\nu}{X}\mathrm{ker}'\right)\frac{\mathrm{kei}}{\Delta} - \left(\mathrm{kei}'' + \frac{\nu}{X}\mathrm{kei}'\right)\frac{\mathrm{ker}}{\Delta} \tag{11a}$$

$$k_{12} = -\left(\mathrm{ker}'' + \frac{\nu}{X}\mathrm{ker}'\right)\frac{\mathrm{kei}'}{\Delta} + \left(\mathrm{kei}'' + \frac{\nu}{X}\mathrm{kei}'\right)\frac{\mathrm{ker}'}{\Delta} \tag{11b}$$

$$k_{21} = -\left[\mathrm{ker}''' + \left(\frac{1}{X}\mathrm{ker}'\right)'\right]\frac{\mathrm{kei}}{\Delta} + \left[\mathrm{kei}''' + \left(\frac{1}{X}\mathrm{kei}'\right)'\right]\frac{\mathrm{ker}}{\Delta} \tag{11c}$$

$$k_{22} = \left[\mathrm{ker}''' + \left(\frac{1}{X}\mathrm{ker}'\right)'\right]\frac{\mathrm{kei}'}{\Delta} - \left[\mathrm{kei}''' + \left(\frac{1}{X}\mathrm{kei}'\right)'\right]\frac{\mathrm{ker}'}{\Delta} \tag{11d}$$

The dependence of these coefficients on the radial crack length a is plotted in Fig. 2(a). Because the structure is elastic, we must of course have $k_{12} = k_{21}$, and the numerical results in Fig. 2(a) show that this is indeed so, although a direct proof from the definition of ker and kei is difficult.

To be consistent with the narrow wedge solution that has l instead of L as the action radius, we further introduce the bending moment and shear force nondimensionalized with respect to l as

$$\bar{M} = \frac{Ml^2}{EI} = \tau^3 k_{11}\bar{\theta}_a + \tau^2 k_{12}w_a; \qquad \bar{V} = \frac{Vl^3}{EI} = \tau^2 K_{21}\bar{\theta}_a + \tau K_{22}w_a \tag{12a,b}$$

where $\bar{\theta} = l\theta = l(dw/dr) = dw/dx$. Based on the solution of (12), the infinite plate for $r > a$ can be treated as a spring support system of the wedge beam.

The solution to the narrow wedge-beam equation (3) has been given by Nevel (1958, 1961) in the following general form:

$$w = c_1\,\mathrm{nev}_0(x) + c_2\,\mathrm{nev}_1(x) + c_3\,\mathrm{nev}_2(x) + c_4\,\mathrm{nel}_1(x) \tag{13}$$

in which $\mathrm{nev}_m(x)$ ($m = 0, 1, 2$) and $\mathrm{nel}_1(x)$ = functions defined by Nevel in terms of the following infinite series:

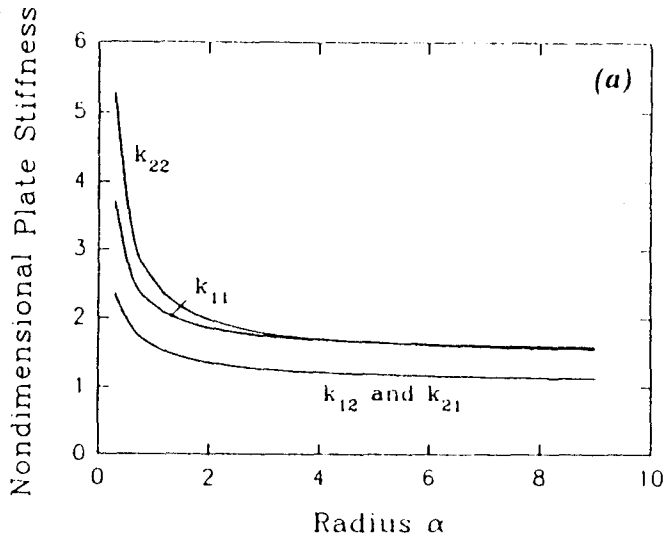

FIG. 2(*a*). Nondimensional Plate Stiffness

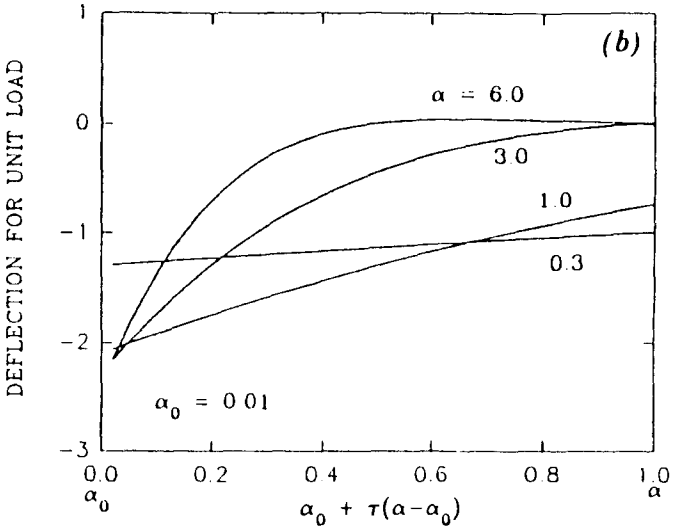

FIG. 2(*b*). Deflection of Wedges

$$\mathrm{nev}_m(x) = x^m + \sum_{k=1}^{\infty} (-1)^k x^{m+4k} \left\{ \prod_{n=1}^{k} [(m + 4n)(m + 4n - 1)^2 \cdot (m + 4n - 2)] \right\}^{-1} \tag{14a}$$

$$\mathrm{nel}_1(x) = \ln(x)\, \mathrm{nev}_1(x) - \sum_{k=1}^{\infty} (-1)^k x^{4k+1} \left\{ \prod_{n=1}^{k} [(4n + 1)(4n)^2 \cdot (4n - 1)] \right\}^{-1} \left[\sum_{r=1}^{k} \left(\frac{1}{4r - 1} + \frac{2}{4r} + \frac{1}{4r + 1} \right) \right] \tag{14b}$$

The boundary conditions for the narrow wedge solution for the end points of the radial cracks are the displacement continuity conditions. This means

that the deflections of the wedge and of the plate must be the same at $r = a$, and that the rotations of the wedges and of the plate at $r = a$ must also be the same. However, when the deflection and rotation of the plate are given, the moment and shear force are determined by virtue of (10). Evidently, the moment and the shear force have to be provided by the wedge. Thus similar equations must be given also for the wedge beam at $r = a$ as follows:

$$\bar{M}_a = \bar{k}_{11} w_a + \bar{k}_{12} \bar{\theta}_a; \qquad \bar{V}_a = \bar{k}_{21} w_a + \bar{k}_{22} \bar{\theta}_a \tag{15a,b}$$

where an overbar means the action radius l is used for the purpose of nondimensionalization. It is easy to verify that $\bar{k}_{11} = \tau^3 k_{11}$; $\bar{k}_{12} = \bar{k}_{21} = \tau^2 k_{12} = \tau^2 k_{12}$; $\bar{k}_{22} = \tau k_{22}$. For the radius of the loaded area ($r = a_0$), the boundary condition can be written as:

$$M = 0; \qquad V = P/2\pi a_0 \tag{16a,b}$$

From these four conditions, the four constants c_i ($i = 1, 2, 3, 4$) can be easily determined. In (16), P is the total force acting on the rim at $r = a_0$. The moment and the shear force can be related to the displacement w as

$$\bar{M} = \frac{Ml^2}{EI} = -\frac{d^2 w}{dx^2}; \qquad \bar{V} = \frac{Vl^3}{EI} = -\frac{1}{x}\frac{d}{dx}\left(x\frac{d^2 w}{dx^2}\right) \tag{17}$$

where $\bar{V}$ and $\bar{M}$ = nondimensional shear force and bending moment per unit width of the wedge.

BEHAVIOR OF SOLUTION

To compare our result with Nevel's, we introduce a nondimensional load $\bar{P} = Pl^2/2\pi EI$, and we assume that $\bar{P}$, rather than P, has a unit value. The deflection curves for a unit nondimensional load and for various values of the relative crack length α are plotted in Fig. 2(b), for the case of a loaded area of relative radius $\alpha_0 = 0.01$. As we see, for short radial cracks ($\alpha - \alpha_0$), the wedge beam behaves like a rigid body. For longer cracks, the bending of the wedge becomes more and more important. For very long cracks (large α), the remote part of the wedge almost does ot deflect (i.e., the effect of the load does not spread beyond a certain distance), which is roughly $\alpha - \alpha_0 = 3$. These features are typical of beams on elastic foundation. For instance, it is known that in a beam of constant cross section on an elastic foundation, the effect of the load does not spread beyond approximately $\alpha = \pi$ (Hetényi 1946; Timoshenko 1959; Selvadurai 1979), which means that a sufficiently long beam can be treated as if it were infinitely long.

The moment distributions in the wedge are plotted under the condition that the bending moment at the boundary of the loaded area ($x = \alpha_0$) is 0. These moment distributions exhibit similar characteristics as the deflections. For a very short wedge beam, the bending moment is almost constant except for a narrow portion near the loaded area (i.e., near $x = \alpha_0$) (see Fig. 3 for different α_0 values). For a very long wedge beam, the bending moments are significant only within the range $x < 3$, beyond which the bending moment is negligible. The nondimensional radius α_0 of the loaded area has a strong effect on the maximum value of the bending moment in the narrow wedge beam. Similar to the solution of an infinite plate loaded over a circle of radius α_0, the smaller the value of α_0, the larger the magnitude of the

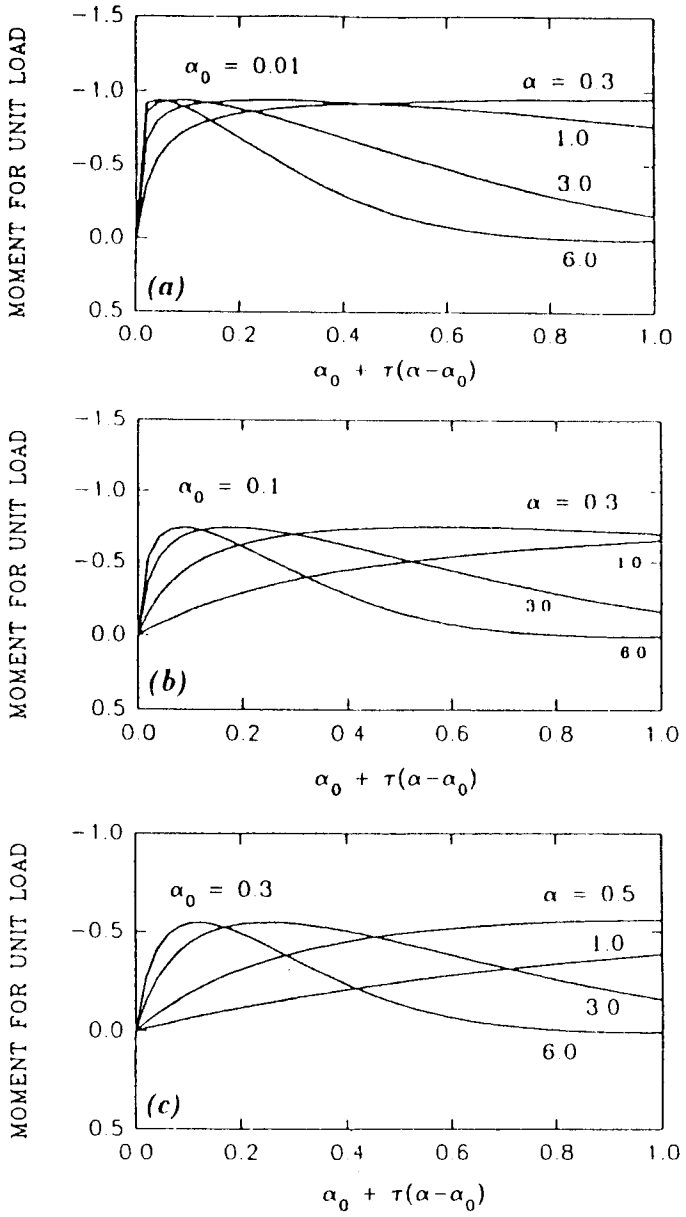

FIG. 3. Moment Distributions of Wedges: (a) with $\alpha_0 = 0.01$; (b) with $\alpha_0 = 0.1$; (c) with $\alpha_0 = 0.3$

maximum negative bending moment (the negative moment is that which causes tension on top of the plate). Furthermore, for a given total applied force, the greater the concentration of the force (i.e., the smaller the value of α_0), the larger the induced bending moments. In other words, the presence of the radial cracks does not change the overall nature of the bending moment distributions.

Nevel (1958, 1961) solved the narrow wedge-beam equation for a beam of infinite length instead of a finite length as we did herein. He assumed the load to be uniformly distributed over the area of the circle of radius α_0. In the present solution, however, it is assumed that the portion of the wedge under the load is chopped off, which means that there is no bending moment at the rim α_0 and the applied load is uniformly distributed as a line load along the rim of all the wedges.

It is useful to realize what is the difference between the foregoing two boundary conditions. The present solution should approach Nevel's solution when $\alpha \to \infty$, which means it should become almost identical when α become sufficiently large. In Nevel's solution the wedge extends all the way to the center and the load is applied uniformly over a circle of radius α_0; in the present paper the load is applied uniformly as a line load over the circumference of this circle. Now, what is the effect of taking away a small portion of the wedge? The effect is quite small and can be neglected. For instance, if $\alpha_0 = 0.01$, the largest deflection for very large α caused by a unit load is about 2.2, while Nevel's result is 2.1. The present result and Nevel's result for the maximum bending moment are both 0.94 for $\alpha_0 = 0.01$, but 0.75 and 0.79, respectively, for $\alpha_0 = 0.1$; they are 0.54 and 0.60 for $\alpha_0 = 0.3$. As we can see, it is only for large diameters of the penetrating object that the difference between the solutions becomes substantial.

It is also interesting to examine the effect of the boundary condition at the rim $x = \alpha_0$ of the penetrating object. We neglect the bending moment at the rim, but in reality, due to rotations, there might be a certain compressive stress near the top of the plate at $x = \alpha_0$. This would produce some positive bending moment on the wedge, which would in turn reduce the magnitude of the negative bending moment in the wedge. Although it is difficult to determine the most realistic boundary condition, it is clear that the results must lie between those for zero bending moment and those for zero rotation at $x = \alpha_0$, the latter case being certainly a gross exaggeration of stiffness. The condition of a free boundary (no bending moment) is conservative as an estimate of the bearing capacity, while the fixed (zero rotation) boundary is conservative as an estimate of the necessary breakthrough load. As one example, numerical calculations show that the extreme negative bending moment is reduced from 0.75 to 0.2 when the boundary condition at $x = \alpha_0$ is changed from a free end to a fixed end, and the location of the extreme bending moment shifts significantly away from the center.

In theory, the present solution with nonzero α_0 should approach Nevel's solution for $\alpha_0 = 0$ when $\alpha_0 \to 0$. Numerically, one finds that the coefficient of $\mathrm{nel}_1(x)$ approaches 0 when $\alpha_0 \to 0$. However, for the condition of zero rim rotation, the numerical solution becomes totally irregular when α_0 becomes less than 10^{-4}, and then the zero rim rotation condition cannot be enforced. From the physical viewpoint, though, this is not surprising, because one can certainly expect that it would be very difficult to hold the wedge beam horizontal at an extremely small α_0 value.

FRACTURE ANALYSIS OF RADIAL CRACK PROPAGATION AND SIZE EFFECT

The solution can always be written in a general form as

$$w = \frac{Pl^2}{2\pi EI} F(x; \alpha_0, \alpha) = \overline{P} F(x; \alpha_0, \alpha) \tag{18}$$

in which $F(x; \alpha_0, \alpha)$ = a nondimensional function. The deflection at the end $x = \alpha_0$ can be written as

$$w_0 = \frac{Pl^2}{2\pi EI} F(x_0; \alpha_0, \alpha) = \frac{Pl^2}{2\pi EI} f(\alpha_0, \alpha) \tag{19}$$

The complementary energy of the structure under load P is

$$\Pi^* = \frac{1}{2} w_0 P = \frac{P^2 l^2}{4\pi E l} f(\alpha_0, \alpha) \tag{20}$$

Energy balance during radial crack propagation requires that

$$nhG_f = \frac{\partial \Pi^*}{\partial a} = \frac{1}{l} \frac{\partial \Pi^*}{\partial \alpha} = \frac{P^2 l}{4\pi E l} \frac{\partial f(\alpha_0, \alpha)}{\partial \alpha} \tag{21}$$

in which n = number of the radial cracks (with uniform angular distribution); and G_f = fracture energy of the material.

In writing the foregoing energy balance condition, we assume that the material follows linear elastic fracture mechanics (LEFM), which is certainly a simplification. In LEFM, the fracture process zone has a zero volume; in reality ice is a quasi-brittle material in which the fracture process zone has a certain finite volume. However, the LEFM solution would be approached asymptotically as the cracks are getting sufficiently long as compared to the size of the fracture process zone.

Eq. (21) involves a second simplification, namely that the frontal edge of the radial crack is a straight line normal to the plate. This assumption is inevitable if the plate theory is used, because the normals are, in this classical theory, assumed to remain straight and normal to the deflection surface. In reality, of course, the frontal edge will not be normal to the plate and there will be a certain region in which the radial crack will penetrate only partially through the plate thickness, growing in the direction normal to the plate. Such crack propagation could be described only by three-dimensional fracture analysis. Again, however, the present solution should become more realistic for longer cracks, which are getting much longer than the length of the region in which the actual crack penetrates only partially through the plate thickness.

From (21) we can solve load P that is necessary to cause radial crack propagation

$$P = 2 \left(\frac{\pi n h E I G_f}{l} \right)^{1/2} \left(\frac{\partial f}{\partial \alpha} \right)^{-1/2} \tag{22}$$

Let us define the nominal stress $\sigma_N = P/h^2$ and the nondimensional nominal stress $\bar{\sigma} = \sigma_N / f_t' = P/h^2 f_t'$, where f_t' = tensile strength of the ice; and denote $g(\alpha_0, \alpha) = 1/[\partial f(\alpha_0, \alpha)/\partial \alpha]^{1/2}$. Provided that $\partial f(\alpha_0, \alpha)/\partial \alpha > 0$, we then have the result

$$\bar{\sigma} = \sqrt{\frac{n\pi E G_f}{3 l f_t'^2}}\, g(\alpha_0, \alpha) = \sqrt{\frac{n\pi l_0}{3l}}\, g(\alpha_0, \alpha)$$

$$= \left(\frac{4\rho}{27} \right)^{1/8} \sqrt{n\pi l_0}\, g(\alpha_0, \alpha) h^{-3/8} \tag{23}$$

in which $l_0 = EG_f/f_t'^2$ = Irwin's characteristic length of the process zone, representing a material length characteristic.

The most interesting aspect of the result in (23) is that, for geometrically similar cracks (same α and α_0, various sizes), the nondimensional nominal stress decreases as $h^{-3/8}$ or as $l^{-1/2}$. This means that there is a size effect.

By contrast, according to all types of strength theory, there is no size effect (Bažant 1992b). For LEFM, as is well known, the size effect in geometrically similar structures is always such that $\bar{\sigma}$ is proportional to $D^{-1/2}$,

in which D = characteristic dimension of the structure. This general property also applies to the present plate bending problem provided that the characteristic dimension of the structure is taken as $D = l$ = flexural wavelength. Normally, however, the characteristic dimension of the structure is taken as one of the geometric dimensions. In the present problem, if the radius of the penetrating object is so small that it is irrelevant, the only geometrical dimension is the plate thickness, h. It is thus quite interesting that the size effect with regard to h is not of the type $h^{-1/2}$ (as a blind application of the general LEFM size effect might suggest) but $h^{-3/8}$. The reason is that the plate thickness is not a dimension of the body in mathematical terms. Rather, due to the buoyancy force serving as an elastic foundation, it is the ratio of beam stiffness to the specific weight of the water, $EI/\rho = l^4$, that provides a characteristic length in the two-dimensional domain.

The fact that the size effect is of the type $h^{-3/8}$ has already been shown by Slepyan (1990) and Bažant (1992b). It is important to note that in term of l, the size effect acquires its familiar form of $l^{-1/2}$ (this was not pointed out in Slepyan's work), so the general scaling law of linear fracture mechanics is preserved. It is also interesting that, as Bažant (1991) proved, the size effect $h^{-3/8}$ applies also to thermal fracture in floating plates caused by critical temperature drop.

The load point compliance $C = w_0/P$ is shown in Fig. 4(a) as a function of α for various values of α_0. The actual value plotted is not the actual compliance C, but function $f(\alpha, \alpha_0)$, which is in direct proportion to C. The compliance monotonically increases with α until it reaches a peak value, after which it starts to show a very small oscillation around the peak level, with a magnitude in the range of 10^{-4}. Such a magnitude of oscillation is so small that it cannot be visually discerned in the plot. Furthermore, the magnitude is decreasing rapidly when α increases. The oscillation of the solution is an intrinsic property of beams on elastic foundation. Nevel (1961) demonstrated that the asymptotic form of the wedge beam solution for large x can be represented by a linear combination of sine and cosine functions modulated by an exponent function of negative exponent. Similar behavior can be found for the functions ker(x) and kei(x) for axisymmetric plates (Watson 1966).

Because $[\partial\Pi^*/\partial\alpha]_P = (P^2/2)(\partial C/\partial\alpha)$, the compliance derivative $\partial C/\partial\alpha$ is a characteristic of the energy release rate due to fracture. The derivative $\partial C/\partial\alpha$ is plotted in Fig. 4(b). We see that it decreases until α reaches approximately 2, after which it becomes zero, which means that the load P required for further crack propagation tends to infinity. In other words, the radial crack propagation is stable for the range of α plotted in the figure; hence, the load required to cause crack propagation cannot be the failure load. After α approaches 2, radial crack propagation is no longer possible. The nondimensional radial crack length at which the compliance first becomes maximized will be denoted as α^*, which is a function of α_0 only. Some typical values are shown in Table 1.

RUPTURE OF WEDGES DUE TO CIRCUMFERENTIAL CRACKS

We will assume the condition of load control, in which case the maximum load is the failure load. The previous section has demonstrated that the load required to drive the radial cracks increases monotonically with the load-point deflection as well as the radial crack length. When α reaches α^*, the corresponding load P will become infinite. Before this can happen, of course,

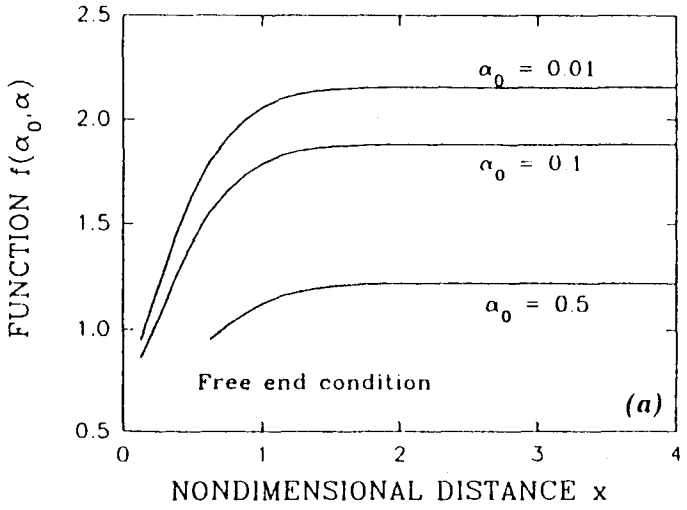

FIG. 4(a). Nondimensional Compliance

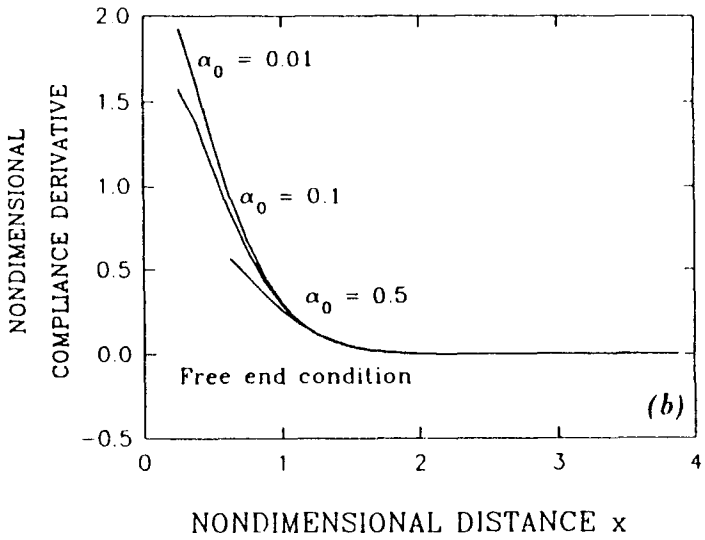

FIG. 4(b). Nondimensional Compliance Derivatives

TABLE 1. Limiting Nondimensional Length of Radial Cracks

(1)	(2)	(3)	(4)	(5)	(6)	(7)	(8)	(9)
α_0	1.0	0.8	0.6	0.4	0.2	0.1	0.05	0.01
α^*	2.43	2.33	2.24	2.16	2.08	2.05	2.03	2.02
$\alpha^* - \alpha_0$	1.43	1.43	1.64	1.76	1.88	1.95	1.98	2.01

the wedges would simply break due to their limited tensile strength. According to the beam theory, the tensile stress of in the top fiber of the wedge is

$$\sigma = -\frac{6M}{h^2} = \frac{6EI}{l^2h^2}\frac{\partial^2 w}{\partial x^2} = \frac{3P}{\pi h^2}\frac{\partial^2 F(x;\, \alpha_0,\, \alpha)}{\partial x^2} \tag{24}$$

where in the last step, the expression (18) for the deflection w is used. Defining the nondimensional nominal failure stress as

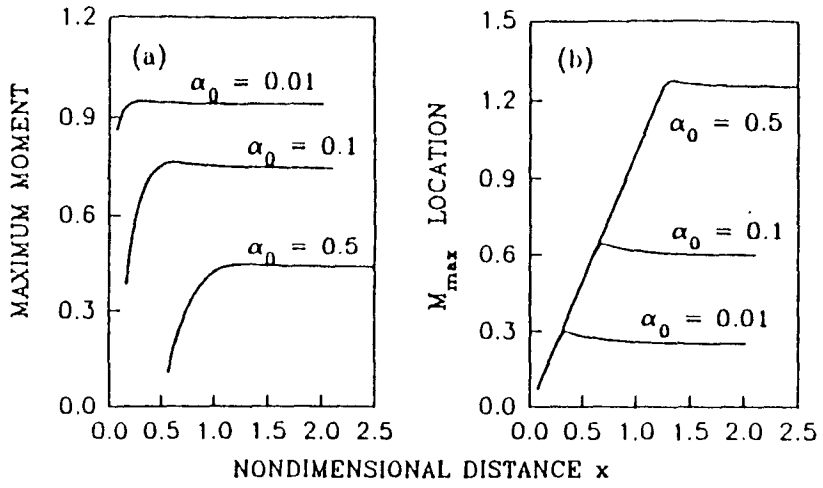

FIG. 5. (*a*) Maximum Nondimensional Moment; (*b*) Location of Maximum Moment

$$\tilde{\sigma}_f = \frac{P}{h^2 f_t} = \frac{\pi}{3F_m(\alpha_0, \alpha)} \tag{25}$$

where

$$F_m(\alpha_0, \alpha) = \max_{x \in [\alpha_0, \alpha]} \left[\frac{\partial^2 F(x; \alpha_0, \alpha)}{\partial x^2} \right] \tag{26}$$

Eq. (25) relates the failure load P for a given α_0 to the radial crack length α. The maximum moments expressed in term of $F_m(\alpha_0, \alpha)$ is plotted in Fig. 5(*a*) and their locations are shown in Fig. 5(*b*). As we can see, for a given α_0, the maximum moment as a function of the radial crack length α increases with α initially, and then reaches a peak value. After that, again F_m starts to oscillate with a very small magnitude around the peak value, similar to the behavior observed for deflection w. The maximum moment in the wedge beam is initially located at the tip of the radial cracks. When it reaches its peak value, however, its location detaches from the crack tip and remains approximately at the same position (in the nondimensional radial distance).

Since the nondimensional nominal stress $\tilde{\sigma}$ required for crack propagation cannot exceed its failure value $\tilde{\sigma}_f$, (i.e., $\tilde{\sigma} < \tilde{\sigma}_f$), the following inequality can be established:

$$\sqrt{\frac{n\pi l_0}{3l}}\, g(\alpha_0, \alpha) \leq \frac{\pi}{3F_m(\alpha_0, \alpha)} \tag{27}$$

This inequality must be satisfied during the process of radial crack propagation, and when this becomes an equality, the wedge will break. The break will be determined by the strength theory, because it occurs at the beginning of formation of the circumferential cracks. This yields an equation to determine the nondimensional crack length α_f at which the wedges break at the location of maximum moment, which does not necessarily lie at the tip of the radial cracks. Eq. (27) can be put into a more compact form as

$$G(\alpha_0, \alpha) \geq n \frac{l_0}{l}; \qquad \text{where } G(\alpha_0, \alpha) = \frac{\pi}{3F_m(\alpha_0, \alpha)} \frac{\partial f(\alpha_0, \alpha)}{\partial \alpha} \tag{28a,b}$$

The function $G(\alpha_0, \alpha)$ is plotted in Fig. 6. From (28) it can be seen that

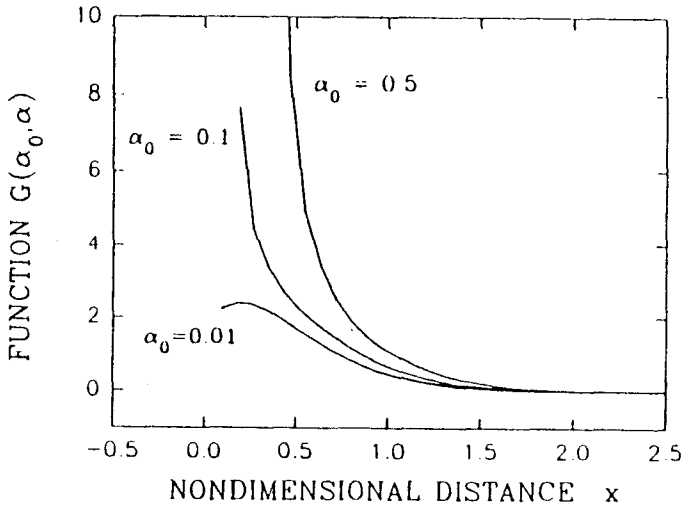

FIG. 6. Function $G(\alpha_0, \alpha)$

the nondimensional radial crack length α at which the wedges would break for a given α_0 depends upon the number of cracks and the ratio of l_0/l. According to some field test data (Frankenstein 1963), n ranges from 3 to 10 for small punch radius a_0, and can reach 30 when the punch radius is large. On the other hand, for typical sea ice, we have $E = 8$ GPa; $f_t' = 1$ MPa; $K_c = 0.1$ MPa $m^{1/2}$, which yields

$$l_0 = \frac{EG_f}{f_t'^2} = \frac{K_c^2}{f_t'^2} = 0.01 \text{ m} \tag{29}$$

The action radii for $h = 0.1$, 0.5, 1.0, and 3.0 m is $l = 2.9$, 9.6, 16, and 37 m, respectively. In all cases, the nondimensional radial crack length $\alpha_f - \alpha_0$ is very close to (although always less than) the maximum value $\alpha^* - \alpha_0$ as listed in Table 1. For instance, when $\alpha_0 = 0.01$, the maximum value of $\alpha^* - \alpha_0$ is 2.01. The estimated radial crack length for $h = 0.1$, 0.5, 1.0, and 3.0 m are about 5.8, 19, 32, and 64 m, respectively. Knowledge of the length of the radial crack at rupture can be very useful in that it provides a measure of how close the applied load is to the failure load (maximum load). Frankenstein (1963) suggested using the formation of circumferential crack as an indicator of failure; however, such an indicator is too close to the final breakthrough. On the other hand, the length of radial cracks provides a quantitative measure of closeness of the applied load to the failure load, therefore seems to be more useful.

Now consider again the size effect. The problem is two dimensional, and the thickness h is not a dimension in the domain of the boundary-value problem. It is merely a parameter. Therefore, the size effect will depend on how the similarity is defined.

First, consider that a_0/h is constant for all the sizes, which is the case of geometric similarity in three dimensions. For this case, the dependence of the nondimensional nominal strength $\tilde{\sigma}_f$ is shown by the solid curves in Fig. 7(*a*). Now it is very interesting to note that, for larger a_0/h, there is a reversed size effect, and for smaller a_0/h there is almost no size effect. The cause for this seemingly strange size effect is that when a_0/h is constant, the value $\alpha_0 = a_0/l$ is increasing with the thickness h. The increase of α_0 then causes a decrease of the magnitude of the maximum negative moment in the wedge beam, which in turn leads to a higher nominal load. However,

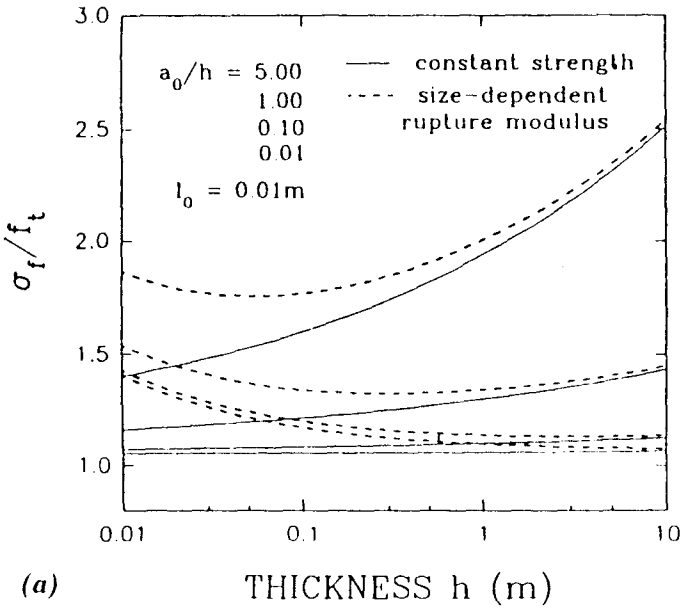

FIG. 7(a). Size Effect of Rupture Loads with Constant a_0/h

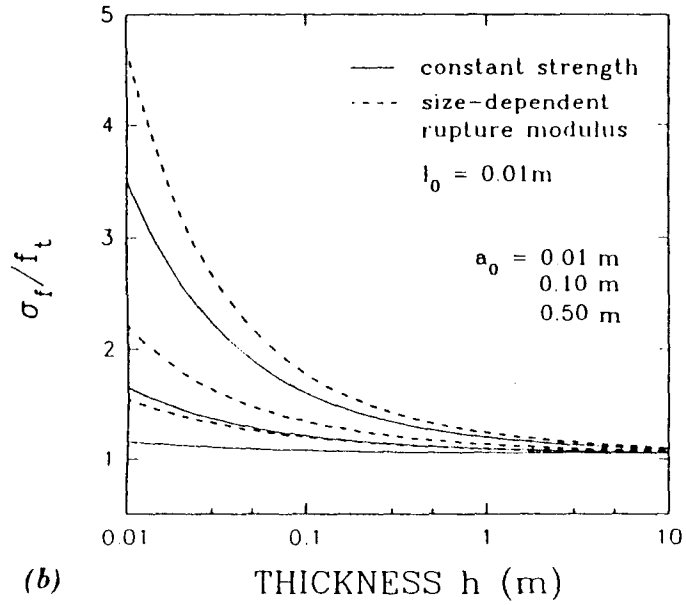

FIG. 7(b). Size Effect of Rupture Loads with Constant a_0

there is another size effect in the apparent value of material strength that will somehow offset this size effect. This size effect arises because the initial nonlinear fracture process zone must develop to a certain finite size before the maximum load is reached, with the peak stress occurring at a certain distance from the top face of the beam rather than at the face. Frankenstein (1963) observed that the formation of circumferential cracks in the ice plate does not lead to immediate breakthrough, in some cases, the final failure would occur until the crack opening at the mouth of the circumferential cracks reaches to a few centimeters. Since polycrystalline ice is a quasi-brittle material, this kind of size effect can be described either by the crack band model (Bažant 1976; Bažant and Cedolin 1979; Bažant and Oh 1983)

or by the fictitious crack model of Hillerborg et al. (1976). Based on the latter, a very simple (although approximate) formula for the size effect on the rupture modulus f_b for bending of quasibrittle materials was proposed by Li et al. (in press, 1994)

$$\eta = \frac{f_b}{f_t'} = 1 + \frac{\sqrt{l_0/h}}{3} \tag{30}$$

where f_t' = uniaxial tensile strength of the ice and f_b is the flexural strength of the ice; $l_0 = EG_f/(f_t')^2$ is a material length. Since l_0 is different for different materials, this equation can be adapted to different types of ice. Using (30), one gets the dashed curves in Fig. 7(*a*), which show that for very small a_0/h there is a normal type of size effect; and for large a_0/h, the opposite size effect still remains. Since l_0 for ice is in the order of a few centimeters, such a size effect is negligible if h is more than 30 cm.

Assuming distributed microcracking, Bažant and Li (1993) proposed another formula: $\eta = 1 + 2l_f/h$, where l_f is an empirical parameter. This formula has also predicted good agreement with test data.

Second, consider that a_0 is constant for all h, in which case there is no geometric similarity in three dimensions. This case is the most relevant to a practical problem in which an aircraft of a fixed and known contact area wants to land safely on an ice plate or a submarine of a fixed and known contact area of its sail wants to penetrate upward through ice. For this case, the size dependence of $\tilde{\sigma}_f$ is shown in Fig. 7(*b*), where the solid curves correspond to the case of constant f_u, and the dashed curves to the case f_u decreasing according to (30). Now we get the normal type of size effect all the size range.

Third, consider that $\alpha_0 = a_0/l$ is constant for all the sizes. This the case of geometric similarity in two dimensions, because the only characteristic dimension presented in the two-dimensional problem is l. In this case there is no size effect if f_u is held constant, because the maximum negative moments in the wedge beam depends only on α_0. The size effect can only originate from the rupture modulus of the ice.

This last property is an interesting feature of the ice penetration problem. In most other failure problems for quasi-brittle materials studied so far, for example the diagonal shear failure, punching shear failure, torsional failure, and bar pull-out failure for concrete structures, the situations at failure are approximately geometrically similar over a broad range of practical cases, but here this is not the case.

It may also be noted that in the present case the size effect can be intensified by the randomness of strength, as described by Weibull statistical theory. This statistical size effect applies only to structures that fail at crack initiation, which is approximately the case for the circumferential cracks. On the other hand, the statistical component of the size effect becomes negligible when the failure occur only after large stable crack growth, as it typically does in concrete structures [as shown by Bažant and Xi (1991)]. In the present problem, large stable growth of radial cracks precedes failure, but the radial cracks do not decide the maximum moment condition; rather, the circumferential cracks do. The Weibull type of statistical size effect in sea ice has been studied by Parsons (1991) and many others. However, the interaction of the statistical strength with the size effect due to development of a large initial fracture process zone in the presence of stress gradient has not yet been studied.

Finally, it should be noted that when the geometric dimension of the

system (such as the thickness of the plate, the size of the punch, and so on) is changed, the number of radial cracks would become different, as was observed by Frankenstein (1963). It is expected that when the number of the radial cracks is different, the maximum moment in the wedge that causes the circumferential cracks is also different, because the central angle of the wedge is different. Thus, there would be a size effect due to a change in the number of radial cracks. This size effect cannot be studied by this simplified version of analysis, because the effect of the wedge angle is ignored by assumption. A detailed study on how to determine the number of radial cracks and the associated size effect will be presented in a subsequent paper (Li and Bažant 1994).

CONCLUSIONS

1. The failure process, which involves propagation of long radial cracks and a maximum load controlled by the initiation of circumferential cracks, can be effectively analyzed on the basis of Nevel's narrow wedge beam approximation, which makes the problem one-dimensional and analytical solution feasible.
2. Geometrical similarity in the present problem means similarity relative to the flexural wavelength $l = (EI/\rho)^{1/4}$, not the plate thickness h.
3. The analysis confirms the recent general result that the size effect on the nominal stress required for crack growth in the sea ice plate is of the type (thickness)$^{-3/8}$, provided that the cracks are geometrically similar.
4. Since in the present case the radial crack propagation is stable, the final failure is not caused by crack propagation. Therefore, the maximum load is not determined by the radial crack growth; rather, it is determined by the initiation of circumferential cracks, which is a strength type of failure.
5. For the practically most important case that the penetrating object has a fixed constant size, there is a size effect in which the nominal strength decreases with increasing size. This size effect is caused by concentration of the applied load. The larger the plate thickness, the smaller is the ratio of the loaded circle diameter to the thickness. The size effect is further intensified by the dependence of the rupture modulus for bending on the plate thickness, which is due to the presence of the process zone. However, this type of size effect is much weaker than that of (thickness)$^{-3/8}$ and disappears for $h \to \infty$.
6. This study demonstrates how the length of the radial cracks is related to the applied load. Also it shows that the final failure would occur when the nondimensional length of the radial cracks approaches approximately twice of the flexural wavelength. Therefore, the length of the radial cracks can be effectively used as a quantitative measure of closeness of the applied load to the maximum load.

ACKNOWLEDGMENT

Financial support under grant N00014-91-J-1109 (monitored by Dr. Y. Rajapakse) from the Office of Naval Research to Northwestern University is gratefully acknowledged.

APPENDIX. REFERENCES

Assur, A. (1956). "Airfields on floating ice sheets for regular and emergency operations." *Tech. Rep. 36; AD 099688*, U.S. Army Snow, Ice and Permafrost Research Establishment (USA SIPRE).

Bažant, Z. P. (1976). "Instability, ductility and size effect in strain softening concrete." *J. Engrg. Mech. Div.*, ASCE, 102(2), 331–344.

Bažant, Z. P., and Cedolin, L. (1979). "Blunt crack band propagation in finite element analysis." *J. Engrg. Mech. Div.*, ASCE, Vol. 105, 297–315.

Bažant, Z. P., and Oh, B.-H. (1983). "Crack band theory for fracture of concrete." *Mat. and Struct.*, Paris, France, Vol. 16, 155–177.

Bažant, Z. P. (1991). "Large scale thermal bending fracture of sea ice plate." *J. Geophysical Res.*, 97(c11), 17739–17751.

Bažant, Z. P., and Xi, Y. P. (1991). "Statistical size effect in quasi-brittle structures. II: Nonlocal theory." *J. Engrg. Mech.*, ASCE, 117(11), 2623–2640.

Bažant, Z. P. (1992a). "Large-scale fracture of sea ice plates." *Proc., 11th IAHR Int. Ice Symp.*, Banff, Alberta, Canada, 991–1005.

Bažant, Z. P. (1992b). "Scaling laws in mechanics of failure." *J. Engrg. Mech.*, ASCE, 119(9), 1828–1844.

Bažant, Z. P., and Li, Z. Z. (1993). "Modulus of rupture: size effect due to fracture initiation in boundary layer." *Struct. Engrg. Rep. No. 93-5/457m*, Dept. of Civ. Engrg., Northwestern University, Evanston, Ill.

Bernstein, S. (1929). "The railway ice crossing." *Trudy Nauchno-Technicheskogo Komiteta Narodnogo Komissariata Putei*, Soobshchenniia, Russia, Vol. 84 (in Russian).

Frankenstein, E. G. (1963). "Load test data for lake ice sheet." *Tech. Rep. 89*, U.S. Army Cold Regions Research and Engineering Laboratory, Hanover, N.H.

Hertz, H. (1884). "Über das gleichgewicht schwimmender elastischer Platten [on the equilibrium of floating elastic plates]." *Wiedemann's Annalen der Phys. und Chem.*, Germany, Vol. 22 (in German).

Hetényi, M. (1946). *Beams on elastic foundation*. University of Michigan Press, Ann Arbor, Mich.

Hillerborg, A., Modéer, M., and Petersson, P.-E. (1976). "Analysis of crack formation and crack growth in concrete by means of fracture mechanics and finite elements." *Cement and Concrete Res.*, Vol. 6, 773–782.

Kerr, A. D. (1975). "The bearing capacity of floating ice plates subjected to static or quasi-static loads—a critical survey." *Res. Rep. 333*, U.S. Army Cold Regions Research and Engineering Laboratory, Hanover, N.H.

Korunov, M. M. (1939). "The calculation of ice crossings." *Avtobronetankovyi Zhurnal*, Russia, (8) (in Russian).

Li, Y. N., and Bažant, Z. P. (1994). "Penetration fracture of sea ice plate: two-dimensional analysis and size effect." *J. Engrg. Mech.*, ASCE, 120(7).

Li, Y. N., Müller, M., and Wörner, J.-D. (1994). "Two new methods of the fictitious crack model and their applications." *J. Engrg. Mech.*, ASCE, (in press).

Nevel, D. E. (1958). "The theory of narrow infinite wedge on an elastic foundation." *Trans. Engrg. Inst. of Can.*, 2(3).

Nevel, D. E. (1961). "The narrow free wedge on an elastic foundation." *Res. Rep. 79*, U.S. Army Cold Regions Research and Engineering Laboratory, Hanover, N.H.

Parsons, B. L. (1991). "The size effect of nominal ice failure pressure, fractals, self similarity and nonstationarity." *11th Int. Conf. on Port and Oc. Engrg. under Arctic Conditions (POAC 91)*, St. John's, Newfoundland, Canada.

Selvadurai, A. P. S. (1979). *Elastic analysis of soil-foundation interaction*. Amsterdam Elsevier Scientific Publ. Co., New York, N.Y.

Slepyan, L. I. (1990). "Modeling of fracture of sheet ice." *Izv. AN SSSR., Mekhanika Tverdogo Tela*, Russia, 25(2), 151–157.

Timoshenko, S., and Woinowsky-Krieger, S. (1959). *Theory of plates and shells*, 2nd Ed., McGraw-Hill, New York, N.Y.

Watson, G. N. (1966). *A treatise of the theory of Bessel functions*, 2nd Ed., The University Press, New York, N.Y.